GU J Sci, Part C, 10(1): 1-14 (2022)

Gazi University

Journal of Science

PART C: DESIGN AND TECHNOLOGY

http://dergipark.gov.tr/gujsc

Microstructure and Mechanical Properties of Silicon Carbide Containing Graphene Platelets Sonicated for Different Times

Sinem BAŞKUT[1*]

[1]*Eskisehir Technical University, Faculty of Engineering, Department of Materials Science and Engineering, 26480, ESKISEHIR*

Article Info

Research article
Received: 23/11/2021
Revision:09/12/2021
Accepted:20/12/2021

Keywords

Graphene Platelets (GPLs)
Sonication Time
Fracture Toughness
Silicon Carbide
SPS

Abstract

Graphene platelets (GPLs) are widely preferred as a second phase to improve the properties of advanced technology ceramics thanks to their excellent mechanical properties. However, their agglomeration tendency requires the application of dispersion processes before mixing with matrix powders. Sonication is the most commonly used technique for the dispersion of GPLs. In this study, the effects of adding GPLs prepared at different probe-sonication times such as 1, 2, 4 and 6 h on the microstructure and mechanical properties of spark plasma sintered (SPS) silicon carbide (SiC) were investigated. Scanning electron microscopy (SEM) examinations and size measurements revealed that the size of GPLs decreased with increasing sonication time. However, the reduction in the size of the GPLs was very low up to the 2 h sonication time and became more pronounced at the GPLs prepared at 4 and 6 h sonication times. Raman analyses indicated that dispersions of GPLs agglomerates increased as well as defects and/or disorders in their structures with increasing sonication time. However, the thickness of the well-dispersed GPLs obtained at the 2 h sonication time did not change when the sonication time was increased to 4 and 6 h. The highest increment in the fracture toughness of SiC matrix in both the through-plane (//) and in-plane (⊥) directions was achieved with the addition of GPLs sonicated for 2 h among the GPLs prepared at different sonication times. The higher contribution of 2 h sonicated GPLs to fracture toughness than non-sonicated and 1 h sonicated GPLs was associated with their more homogeneous distribution in the matrix microstructure, while higher toughness values they provided compared to 4 and 6 h sonicated GPLs could be explained by the positive effect of their higher lateral size and aspect ratio. GPLs have improved the fracture toughness of SiC matrix with the help of bridging and deflection toughening mechanisms.

1. INTRODUCTION

In recent years, graphene platelets (GPLs), a two-dimensional form of carbon, have been attracted attention as the second phase in improving the mechanical properties of advanced technology ceramics, thanks to their high surface area and superior mechanical properties (high fracture strength (~125 GPa) and Young's modulus (~1TPa)) [1-3]. SiC as an important member of the advanced technology ceramics group, has a combination of excellent properties such as high hardness and strength, corrosion and oxidation resistance, chemical and thermal stability, and melting point. These properties of SiC have provided to be used in high temperature, wear resistant and cutting applications in many industrial areas such as automotive and aerospace industries [4-6]. However, the low fracture toughness of SiC restricts its usage areas.

It has been determined that the mechanical properties of matrix materials have increased significantly with the addition of GPLs [7-15]. In a study [7] in which GPLs-SiC composites were produced with the SPS technique at different temperatures, it was observed that the fracture toughness of SiC improved by approximately 5-20 % with the addition of 1 wt % GPLs. Li et al. [8], who sintered the SiC matrix composites containing 0.5, 1 and 1.5 wt % GPLs by using vacuum reaction sintering furnace, achieved the highest strength and fracture toughness at 1 wt % GPLs content with an increase of ~ 50 %. In a different study [9], the fracture toughness of SPSed SiC was improved by ~ 40 % with the addition of 2 wt % GPLs. Yang et al. [10], sintered the Si_3N_4 matrix composites containing 0.2, 0.5, 1, 2, 5 and 10 wt % GPLs using

*Corresponding author, e-mail: skayhan@eskisehir.edu.tr
DOI:10.29109/gujsc.1027462

the hot pressing technique determined that there was an improvement of ~ 10 and 3 % in the fracture toughness and strength of the Si_3N_4, respectively, at 0.2 wt % GPLs content.

The distribution of GPLs in the matrix microstructure is one of the critical parameters that affect the properties and performance of the final composites. For high mechanical performances, the GPLs should be homogeneously dispersed within the matrix microstructure without any agglomeration [16]. The fact that the GPLs tend to agglomerate due to weak van der Waals interactions between them indicates the importance of the applied dispersion techniques. It was determined that sonication is the most common and effective method used to dispersion of the GPLs before mixing with matrix powders. Sonication can be performed to the liquid containing GPLs in two ways, ultrasonic bath and probe-sonicator. The sound waves applied during sonication causes to agitate the GPLs in a liquid medium. In this way, the GPLs in the outer part of agglomerates peel off and become individual sheets [11]. Porwal et al. [12], who produces graphene reinforced alumina nanocomposites by using the SPS technique, have dispersed the GPLs for 2 h by sonication technique and then blended them with the alumina starting powders for 4 h using ball milling. In another study [13] which GPLs-aluminum nitride (AlN) composites were sintered by hot pressing technique and the mechanical properties of the products were measured, GPLs were first sonicated for 1.5 h and then mixed with AlN powders by using a planetary mill. To produce GPL-Si_3N_4 composites, Tapaszto et al. [14] applied 30 min of sonication to GPLs following the 30 min of planetary milling in the presence of melamine and blended the sonicated GPLs with Si_3N_4 powders by mechanical milling.

In all these studies, GPLs were dispersed for different sonication times before mixing with matrix powders. However, no study was found to determine the sonication time that would maximize the mechanical properties of the matrix to which GPLs were added. Additionally, it has been reported that the probe-sonication was more efficient in the dispersion of agglomerates than bath sonication [17]. Therefore, the motivation of this study was to determine the sonication time which GPLs can be successfully dispersed with minimal structural damage since the sonication process was known to cause defects/disorders in the structure and surface of the GPLs [18] and to investigate the effects of the addition of GPLs prepared at different sonication times on the microstructure and mechanical properties of SiC matrix such as hardness and fracture toughness. For this purpose, GPLs were prepared with probe-sonication technique for 1, 2, 4 and 6 h. SiC matrix and GPLs-SiC composites were sintered using the SPS technique. Microstructure, density, hardness, and fracture toughness measurements of the produced materials were carried out.

2.MATERIALS AND METHODS

Commercially available α-SiC powder (Saint Gobain Sika, DENSITEC 15) containing B_4C (CRS Chemicals, F2000 Grade) at a ratio of 1 wt % was used as starting material. Y_2O_3 (99.9% purity, H.C. Starck Berlin, Germany) and Al_2O_3 (Alcoa-A16SG) powders were used as sintering additives. The matrix material consists of the 93 wt % α-SiC, 5 wt % Y_2O_3 and 2 wt % Al_2O_3. ~ 12.2 μm average lateral size, 5-8 nm thickness and 99.9 % purity were the properties of the commercial GPLs (Graph. Chem. Ind. Comp.) used during the study. The amounts of starting powders that form the SiC matrix and GPLs-SiC composites are given in Table1.

Table 1. *The amounts of starting powders that form the SiC matrix and GPLs-SiC composites*.

Starting Powders	***Compositions (g)***	
	SiC Matrix	*GPLs-SiC Composites*
SiC	*27.9*	*27.62*
Y_2O_3	*1.50*	*1.49*
Al_2O_3	*0.60*	*0.59*
GPLs	*-*	*0.3*
Total	***30***	***30***

Probe-sonication was applied to GPLs in the isopropanol medium for 1, 2, 4 and 6 h under the conditions of successive vibration for 16 s and standby for 25 s, at the 20 kHz frequency, 40 % of amplitude. Sonication processes were carried out in an ice bath to avoid the negative effects of heat on the structure and surface of GPLs. The sizes of the GPLs were measured (Malvern Instruments, Hydro 2000) after each sonication process. The SiC, Y_2O_3 and Al_2O_3 powders were blended in the planetary ball mill by using the Si_3N_4 medium and Si_3N_4 balls for 1 h at 300 rpm. Non-sonicated GPLs and GPLs prepared at different sonication times were added to the matrix material composition at a rate of 1 wt %, and mixing was continued with planetary ball mill for 1 h at 120 rpm in the isopropanol medium. The evaporator removed the isopropanol in the slurries and the obtained GPLs-SiC composite powders were sieved. The SiC matrix and GPLs-SiC compositions were sintered using the SPS technique (HP 25D, FCT GmbH) at 1950 and 2000 °C, respectively. Sintering of all samples carried out at 50 MPa uniaxial pressure for 4 min under a vacuum atmosphere.

The samples' bulk density values were measured using the Archimedes method in the deionized water as the immersion medium. The relative density values were calculated by the rule of mixtures. The theoretical densities of SiC and GPLs were used as 3.21 and 2.26 gcm^{-3}, respectively during the calculations. Samples were cut parallel and perpendicular to the SPS pressing axis since several studies have reported that the uniaxial pressure applied in the SPS causes the GPLs to be oriented within the matrix microstructure. The investigation and measurement directions were called through-plane (//, parallel to the SPS pressing axis) and in-plane (⊥, perpendicular to the SPS pressing axis) directions. The cutting and examination details were given elsewhere [19].

The cut samples were polished from coarse to fine with diamond polishing solutions and appropriate polishing cloths in the automatic polisher (STRUERS, TegraPol-25). XRD (Rigaku, RINT-2000) analyses were carried out in the through-plane (//) direction between 20 and 80° (2Θ), at 40 kV accelerating voltage, 30 mA current, 2°/min scan speed and 0.02 step size since a distinctive graphene peak was obtained in this direction [19]. The Raman (WITec, alpha 300) analyses were performed to each GPLs prepared at different sonication times.

The hardness values of the samples were measured by using the Vickers indentation (Emco-Test) technique under the conditions of 5 kg load and 10 s dwell time. At least five measurements were performed for each sample, and average values were used to obtain statistical results. Furthermore, the fracture toughness values were calculated by using the equation 1 given below [20]:

$$K_c = 0.067 \left(\frac{E}{H_V}\right)^{0.4} H_V \alpha^{0.5} \left(\frac{c}{a}\right)^{-1.5} \quad (1)$$

While the morphologies of the GPLs were examined by secondary electron (SE-SEM) imaging technique, the polished and indented surfaces of the sintered samples were investigated by backscatter electron (BSE-SEM) imaging technique in the SEM (Zeiss, SUPRA 50 VP).

1. RESULTS AND DISCUSSION

Figure 1 shows morphological SE-SEM images of the non-sonicated GPLs (a) and GPLs sonicated for 1 (b) , 2 (c), 4 (d) 6 (e) h. Additionally, the GPLs platelet sizes, measured after each sonication process are given in Table 2. Morphological images and platelet size measurements were compatible with each other, and they demonstrated that the platelet size of GPLs decreased as the applied sonication time increased. Measurements indicated that the size of the non-sonicated GPLs, which was about 12.20 µm, reduced by ~ 2, 5, 25 and 30 to 11.90, 11.55, 9.10 and 8.50 µm with probe-sonication for 1, 2, 4 and 6 h, respectively (Table 2). This revealed that the GPLs undergo fragmentation as well as dispersion due to the generation of shear force caused by shock waves during the sonication process [18]. However, there was a very slight decrease in the average platelet sizes of GPLs sonicated for 1 and 2 h, while the decrease has became

evident when the sonication time was increased to 4 and 6 h. Although the size difference was large among the non-sonicated GPLs, GPLs sonicated for 6 h had a more uniform platelet size distribution (Fig. 1).

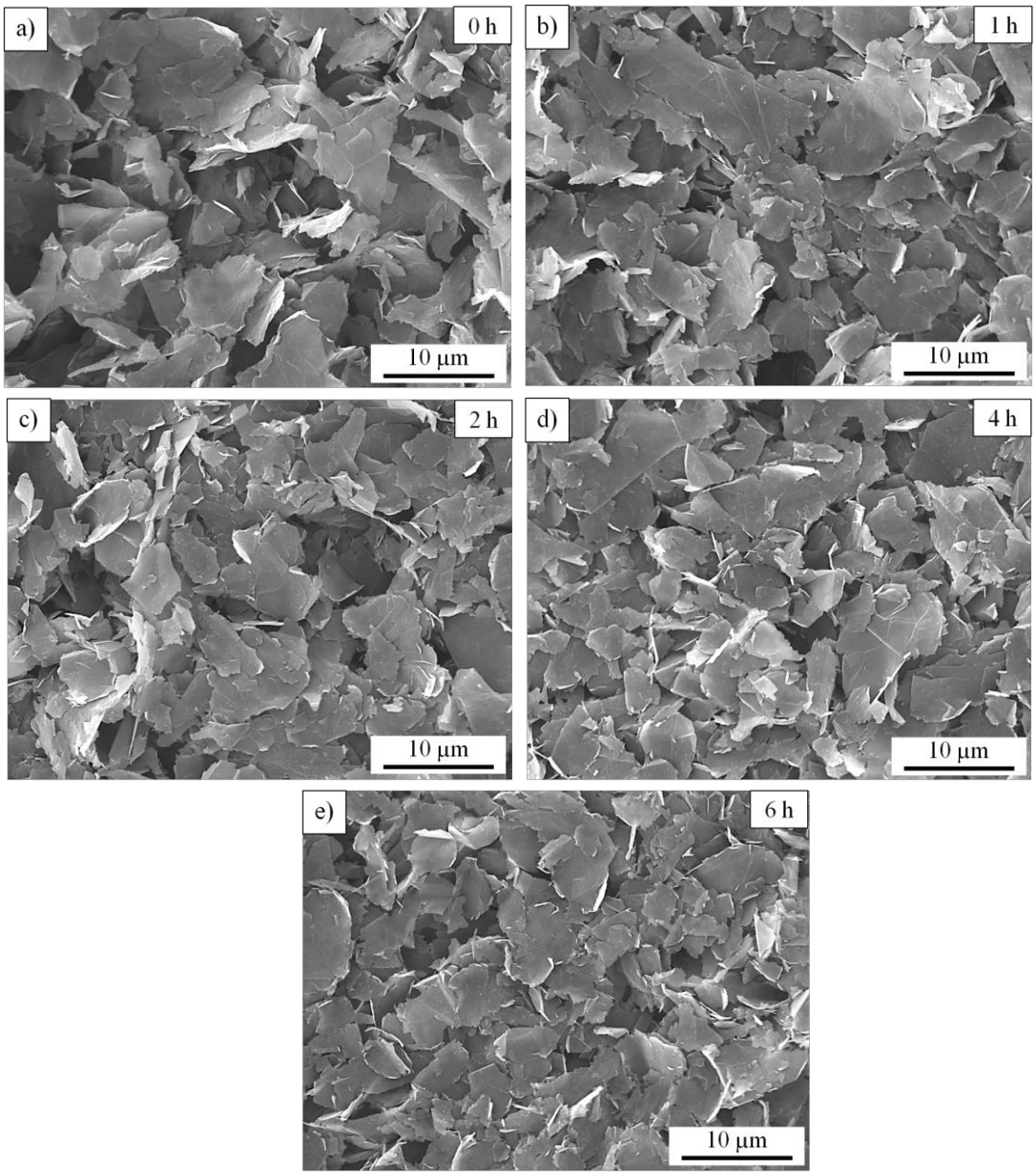

Figure 1. *Morphological SE-SEM images of the (a) non-sonicated GPLs and GPLs sonicated for (b)1, (c) 2, (d) 4 and (e) 6 h.*

Figure 2 and Table 2 present the Raman spectra and Raman analysis results of non-sonicated GPLs and GPLs sonicated at different times, respectively. The single shape of the 2D band in the spectra of all GPLs (Fig. 2) confirmed the graphene phase [21]. 2D-band generally related to the thickness of the GPLs, and the ratio of the 2D-band intensity to the G-band intensity (I_{2D}/I_G) gives information about the number of layers [22, 23]. During the study, at least ten Raman analyses were performed to each GPLs, and the averages of the obtained values were given in Table 2. The average I_{2D}/I_G value (0.880) and measurement ranges (0.755–0.960) indicated that non-sonicated GPLs were multilayered in different thicknesses. With the application of probe-sonication for 1, 2, 4 and 6 h, the average I_{2D}/I_G value increased to 0.905, 0.937, 0.940, and 0.942, respectively. These results revealed that the stacked GPLs were de-agglomerated with sonication and that the thickness of the GPLs decreased with increasing processing time. The fact that the

lowest measured I_{2D}/I_G limit increased as the applied sonication time increased showed that the dispersion of GPL agglomerates continued with increasing sonication time. On the other hand, the upper I_{2D}/I_G limit remained the same as the time increased after 2 h of sonication (Table 2), indicating that the thinnest GPLs that could be obtained by sonication was achieved at this point, and no further thinning could occur as the process continued.

Table 2. *The average sizes of the non-sonicated GPLs and GPLs sonicated at different times and also average I_{2D}/I_G, I_D/I_G values calculated by using at least ten Raman analyses. The values in brackets are for the measurements range*

Sonication Time (h)	***Average Size (μm)***	***I_{2D}/I_G***	***I_D/I_G***
0	*12.20*	*0.880 (0.755–0.960)*	*0.847 (0.769–0.895)*
1	*11.90*	*0.905 (0.782–0.967)*	*0.855 (0.786–0.900)*
2	*11.55*	*0.937 (0.855–0.981)*	*0.870 (0.803–0.906)*
4	*9.10*	*0.940 (0.870–0.981)*	*0.884 (0.815–0.917)*
6	*8.50*	*0.942 (0.890–0.982)*	*0.892 (0.823–0.926)*

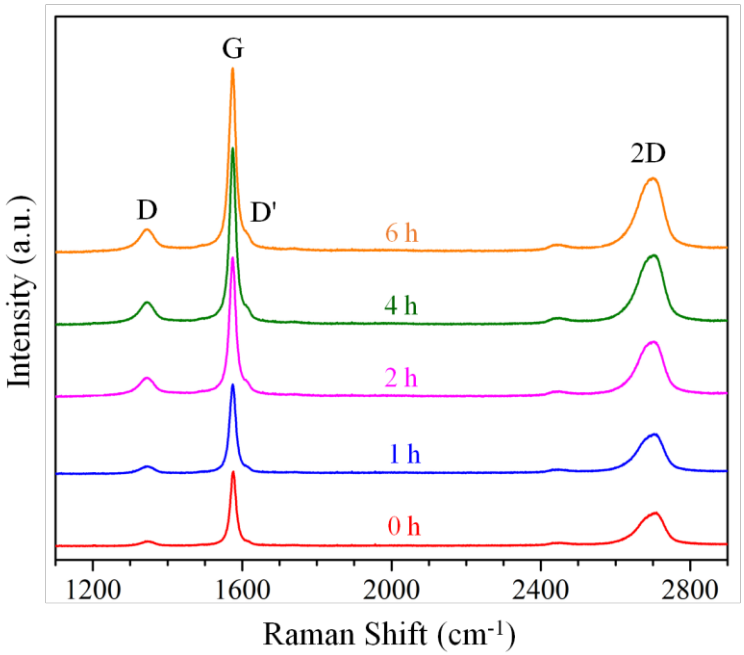

Figure 2. *Raman spectra of the non-sonicated GPLs and GPLs sonicated for 1, 2, 4, 6 h.*

The ratio of the D-band intensity to the G-band intensity (I_D/I_G) in the Raman spectra can be used to express the degree of defects and disorders in the GPLs structure [23]. As seen in Table 2, the ratio of I_D/I_G increased with increasing probe-sonication time. The fact that the increased degradation in the GPLs structure has a negative effect on their reinforcement strength [16] has shown the necessity of achieving maximum dispersion in short sonication times.

Table 3 gives the bulk and relative density values of SiC matrix and SiC matrix composites containing GPLs. The bulk and relative densities of the SiC matrix were determined as 3.205 gcm^{-3} and 99.8 %, respectively. This showed that the applied sintering conditions were suitable for obtaining highly dense SiC. On the other hand, with the addition of GPLs prepared at different times, the bulk density of SiC

decreased by about 2 %. Porosities that may occur in the composite microstructure and cracks formation in the layered structures caused by the thermal expansion and elastic modulus mismatch between GPLs and the matrix can be shown as the reasons for this decline in density [24, 25]. The relative densities of GPLs-SiC composites higher than 97 % showed that high-density composites were produced in themselves.

Table 3. *Bulk and relative density values of the SiC matrix and SiC matrix composites containing non-sonicated GPLs and GPLs prepared at different probe-sonication times.*

Sonication Time (h)	***Bulk Density (gcm^{-3})***	***Relative Density (%)***
SiC Matrix	*3.205*	*99.8*
0	*3.125*	*98.2*
1	*3.115*	*97.9*
2	*3.120*	*98.1*
4	*3.120*	*98.1*
6	*3.100*	*97.4*

The through-plane (//) direction XRD pattern (Fig. 3) obtained from the SiC matrix and GPLs-SiC composites showed the presence of two main hexagonal polytypes of SiC, 6H-SiC and 4H-SiC. During sintering, the 6H-SiC structure was partially transformed to 4H-SiC [26]. The low intensity graphene peak determined at 26.6 degrees in the pattern of SiC matrix indicated that the free carbon contained in the initial SiC powder crystallized during SPS. The intensity of the graphene peak increased with the addition of GPLs.

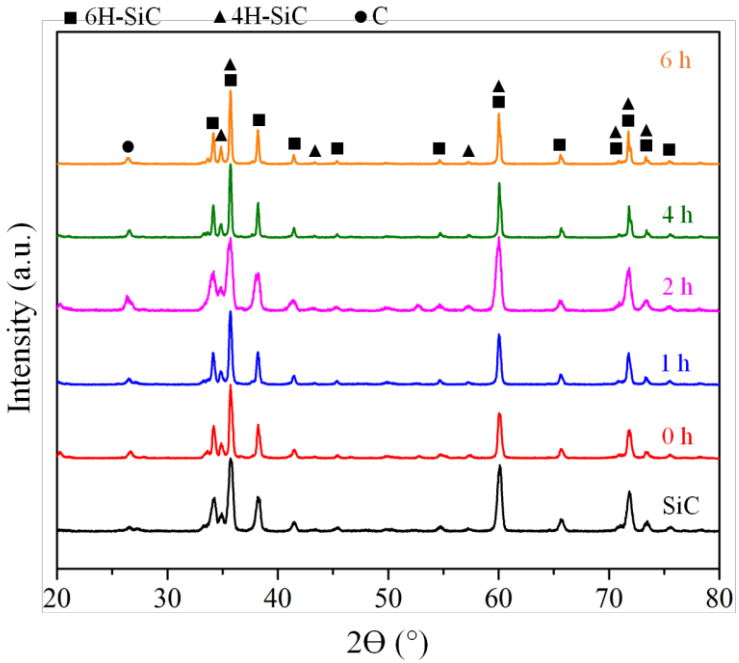

Figure 3. *Through-plane (//) direction XRD pattern obtained from the SiC matrix and SiC matrix composites containing non-sonicated GPLs and GPLs sonicated for 1, 2, 4 and 6 h.*

Figure 4 presents low (a, c, e, g, i, k) and high (b, d, f, h, j, l) magnification BSE-SEM images of SiC matrix (a, b) and GPLs-SiC composites (c-l) taken in the in-plane (⊥) direction. To investigate whether black phases that are needle and spherical like observed in the microstructure of SiC matrix are porosity or not, magnified BSE-SEM and in-lens-SEM images obtained from the same region are given in Figure 5 a and b, respectively. The in-lens-SEM image, a surface sensitive imaging technique, revealed that the phases marked with arrows in the BSE image were not porosities. The needle-like phase indicated by the blue arrows may be associated with the crystallized carbon identified in XRD, while the spherical-like phase (indicated with pink arrows) may be the crystallized carbon or B_4C phase whose source was B_4C powder contained at the small amount in the starting powder mixture. In addition, the regions indicated by yellow arrows demonstrated that some crystallized carbon or B_4C grains were pulled out from the surface during mechanical polishing. The homogeneous dispersion of the SiC grains, white liquid phase and black phase associated with crystallized carbon and/or B_4C without any porosity in the microstructure of the SiC matrix supported the density result by showing that a highly dense SiC matrix was produced.

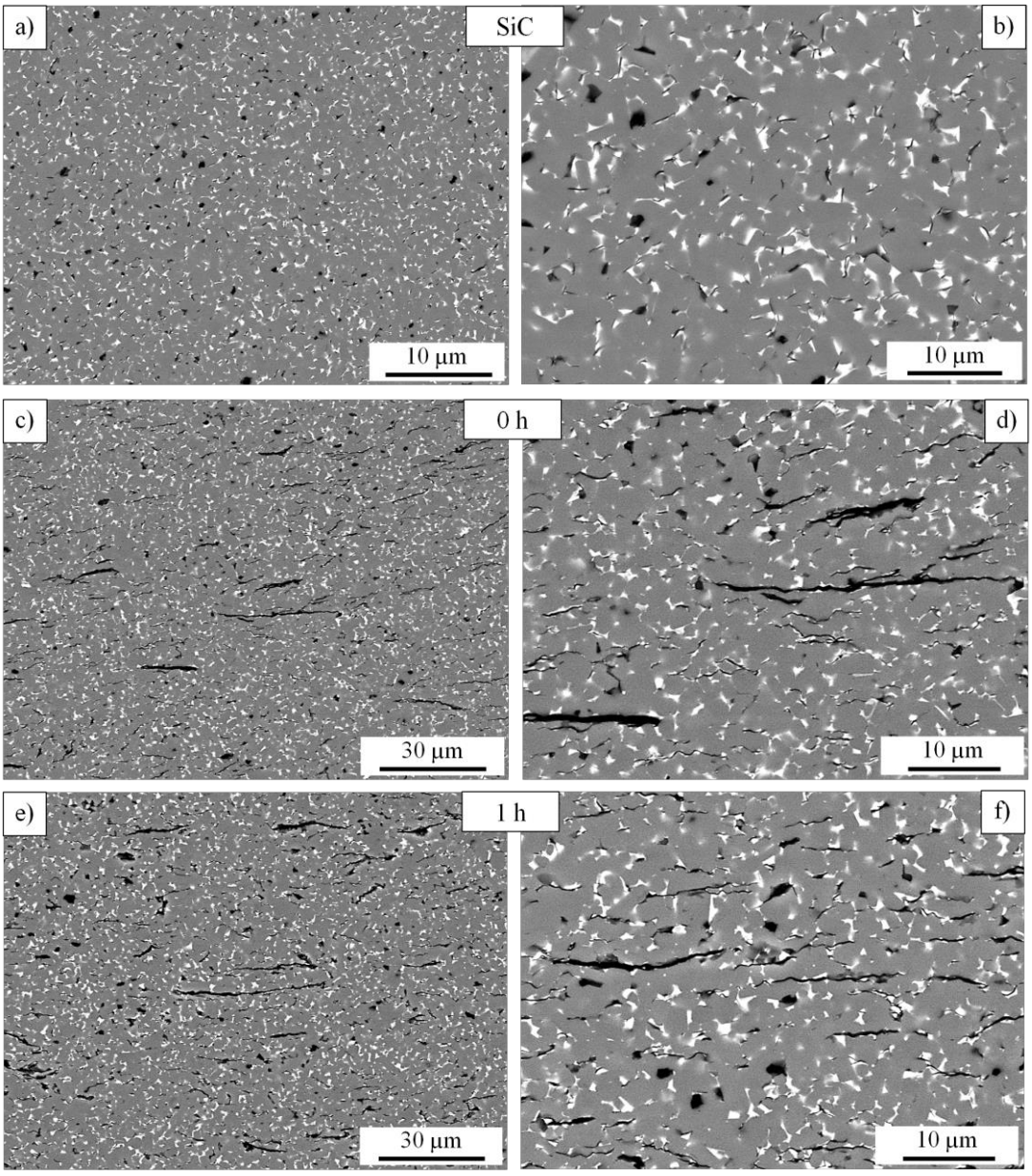

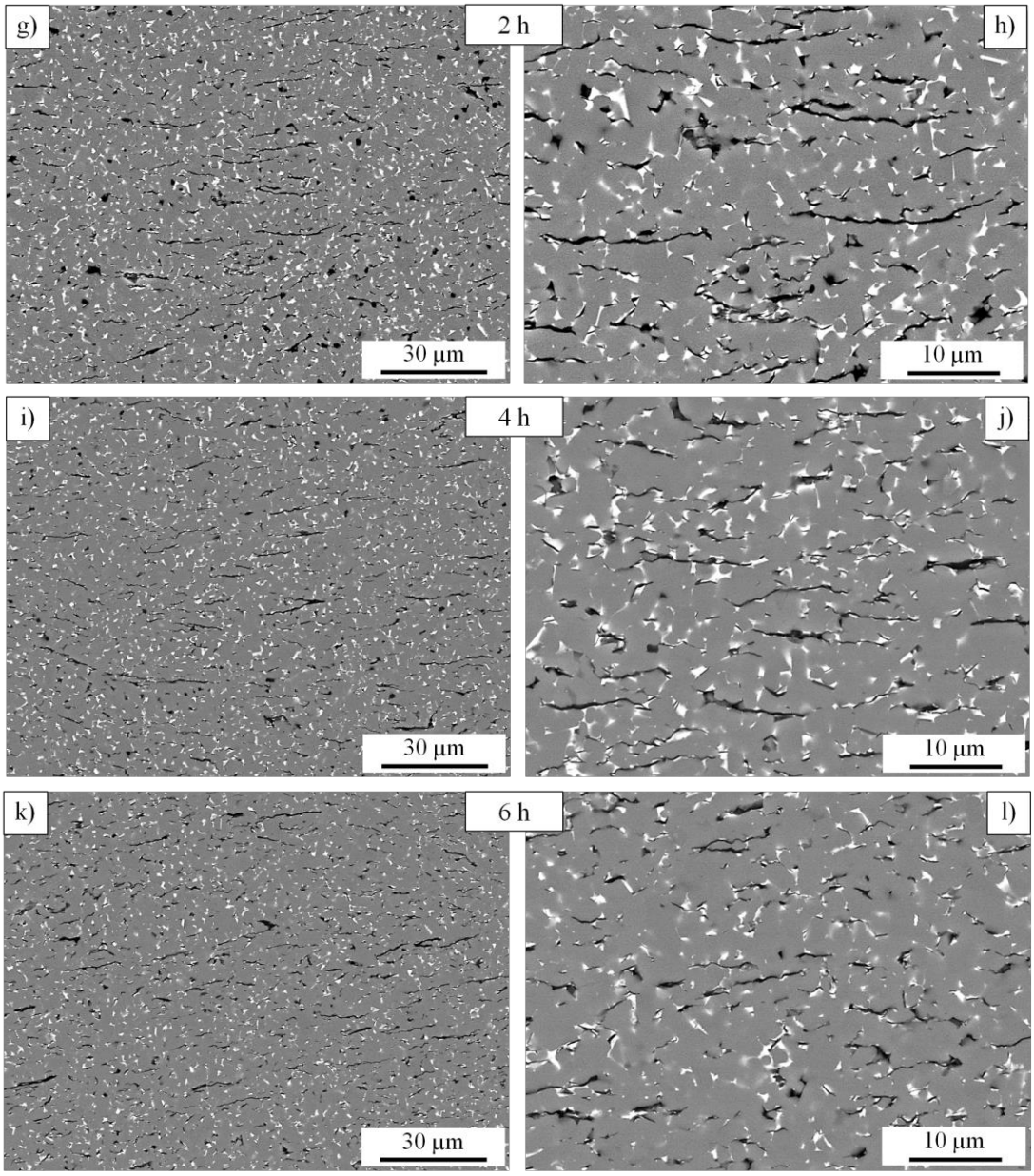

Figure 4. *BSE-SEM images taken at low and high magnifications from (a, b) SiC matrix and SiC matrix composites containing (c, d) non-sonicated, (e, f) 1, (g, h) 2, (i, j) 4, (k, l) 6 h sonicated GPLs.*

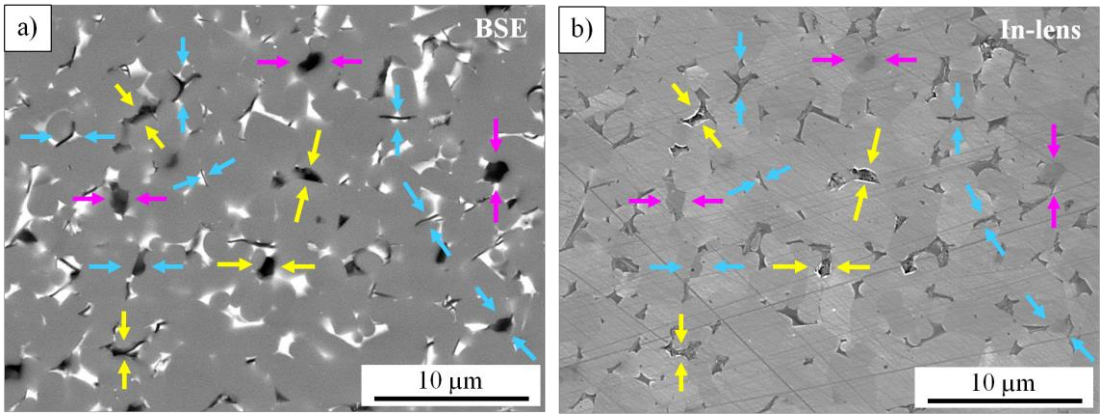

Figure 5. *(a) BSE-SEM and (b) in-lens-SEM images obtained from the same region of the SiC matrix.*

It was clear that the GPLs represented by black color were dispersed with orienting in the microstructure of the GPLs-SiC composites (Fig. 4 c-l) due to applied uniaxial pressure in the SPS. Additionally, while no significant change was observed in the size of the GPLs at the 1 and 2 h sonication times, a noticeable size reduction has occurred in the 4 and 6 h sonicated GPLs as consistent with size measurement results.

Besides, the microstructures demonstrated the presence of thick GPLs in non-sonicated and 1 h sonicated GPLs, and also showed that these stacked structures were highly dispersed in 2, 4 and 6 h sonicated GPLs. However, there was no significant difference in thickness between the GPLs sonicated for 2, 4 and 6 h. When the microstructures of all produced GPLs-SiC composites were evaluated together, it was determined that the presence of thicker GPLs in the non-sonicated GPLs limited their homogeneous distribution in the matrix microstructure compared to the sonicated GPLs. The applied sonication processes have enabled the dispersed GPLs to be homogeneously distributed in the SiC matrix microstructure. Measurements and microstructural studies have shown that GPLs could be effectively dispersed and retain their sizes without much fragmentation at 2 h sonication time. In addition to all these, microstructures have shown that high-density GPLs-SiC composites could be produced.

The effects of adding the GPLs dispersed at different probe-sonication times on the hardness and fracture toughness of the SiC matrix are shown in Figure 6. Since no significant difference was observed between the samples' through-plane and in-plane directions hardness values, the averages of the values measured in both directions were used. The hardness of the SiC matrix was reduced by ~ 8 and 7, 6, 5, 5 with the addition of 1 wt % non-sonicated GPLs and 1, 2, 4, 6 h sonicated GPLs, respectively. Weak interfacial bonding between GPL agglomerates and SiC grains could be accepted as a reason for this decline. As the applied sonication time increased, the degree of dispersion of the agglomerates also increased, and the decline in the hardness of SiC relatively decreased (Fig. 6 a).

The fracture toughness of the SiC matrix did not exhibit a noticeable difference between the through-plane and in-plane directions like the hardness value. GPLs sonicated at different times improved the fracture toughness of the SiC matrix at different degrees in both directions. The fracture toughness of the SiC matrix (5 MPa $m^{1/2}$) increased by ~ 4, 12, 28, 26, 24 % and by ~ 12, 22, 38, 30, 28 % in the through-plane and in-plane directions, respectively, with the addition of non-sonicated, 1, 2, 4, 6 h sonicated GPLs. In both the through-plane and in-plane directions, the highest fracture toughness value was achieved with the GPLs sonicated for 2 h, while the non-sonicated GPLs provided the least enhancement (Fig. 6 b). Figure 7 shows the BSE-SEM images of the representatively selected cracks obtained by in-plane direction indentations in SiC matrix and 2 h sonicated GPLs-SiC composites. It was seen that black phases associated with crystallized carbon and/or B_4C also play an important role in the dissipation of the energy accumulated at the tip of the crack formed in the SiC matrix in addition to the grain boundaries (Fig. 7 a). Crystallized carbon and B_4C grains preserved the fracture toughness of the matrix mainly by the bridging mechanism (indicated with yellow arrows). On the other hand, the energy of the crack formed in SiC containing 1 wt % GPLs sonicated for 2 h (Fig. 7 b) decreased under the influence of the bridging and deflection toughening mechanisms (indicated with green arrows) provided by GPLs as well as the bridging mechanism of the black grains associated with crystallized carbon and B_4C (indicated by yellow arrows); thus, the crack has thinned and stopped.

The lowest toughness value of the SiC containing non-sonicated GPLs among the produced GPLs-SiC composites can be explained by the formation of GPLs-rich and GPLs-poor regions in the matrix microstructure due to undispersed GPLs agglomerates (Fig. 4 c). Since the contribution of GPLs to preventing or retarding crack propagation was limited in GPL-poor regions, the toughness values in the measurements corresponding to these regions were close to that of the SiC matrix. As a result of the dispersion of the GPLs by the applied sonication processes, their more homogeneous dispersion compared to the non-sonicated GPLs in the matrix microstructure led to more improvement on fracture toughness. The fracture toughness tended to increase up to the composite containing GPLs sonicated for 2 h, whereas it started to decrease when the sonication time was increased to 4 and 6 h. The increase in the toughness of SiC matrix by the GPLs sonicated for 2 h more than the 1 h sonicated GPLs can be explained by the fact

that the crack has a greater chance of encountering homogeneously distributed GPLs, thus the activation of more toughening mechanisms.

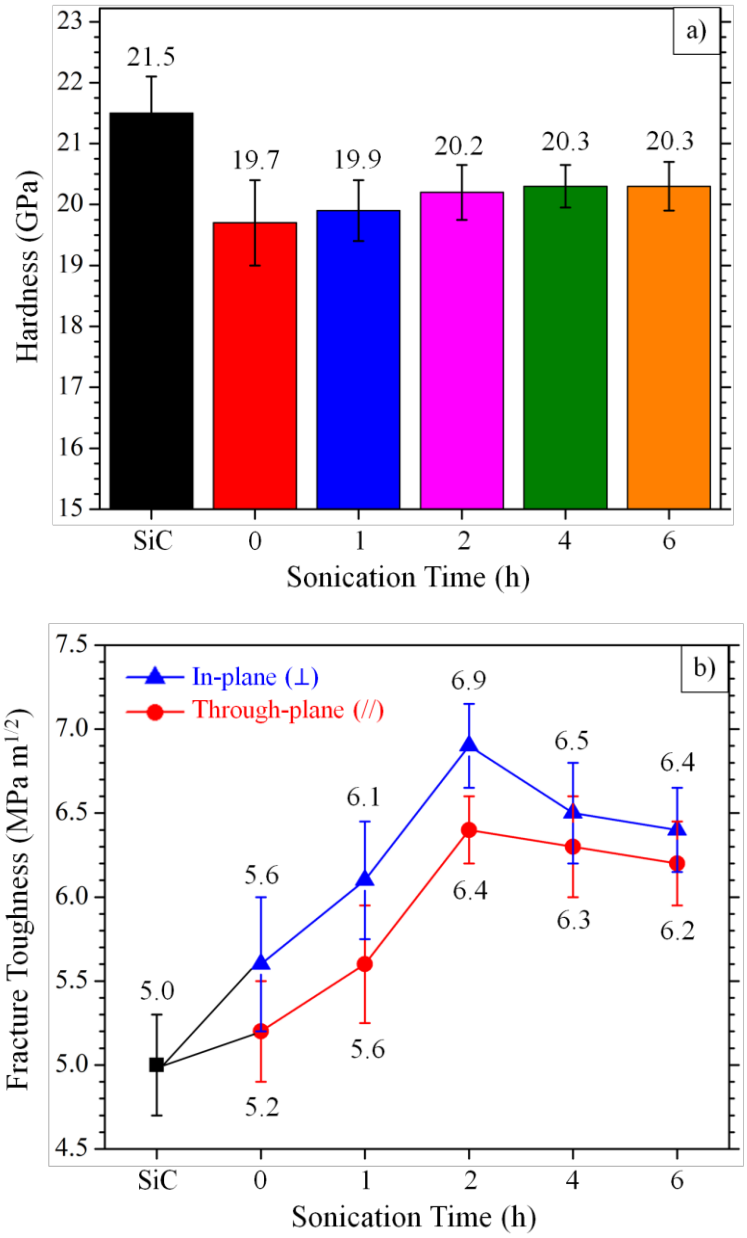

Figure 6. *(a) Hardness and (b) fracture toughness values of the SiC matrix and GPLs-SiC composites.*

The higher fracture toughness of SiC containing GPLs sonicated for 2 h compared to the SiCs containing GPLs prepared at 4 and 6 h indicated the positive effect of the large lateral size of GPLs on fracture toughness. Larger GPLs were more successful than smaller ones at retarding crack propagation by mechanisms such as deflection and bridging. This result was compatible with the study [27] in which the mechanical properties of polymer matrix composites containing two different GPLs with lateral sizes of 5 and 25 µm at the same thickness were measured. In that study, at the same GPLs contents, the fracture toughness and flexural modulus values of the composites containing GPLs having 25 µm lateral size were found to be significantly higher than those containing a GPLs with a size of 5 µm. Furthermore, this different fracture toughness behavior of SiCs containing GPLs sonicated for 2, 4 and 6 h can also be associated with the different aspect ratios of GPLs. As the Raman and microstructure analyses revealed that

there was no obvious thickness difference between GPLs sonicated for 2, 4 and 6 h and the platelet size of the 2 h sonicated GPLs was larger than the others, it can be assumed that the GPLs sonicated for 2 h had the highest aspect ratio among these three GPLs. GPLs with a high aspect ratio bond more strongly with the matrix than GPLs having a low aspect ratio, facilitating the transfer of load from the matrix to the GPLs [28, 29].

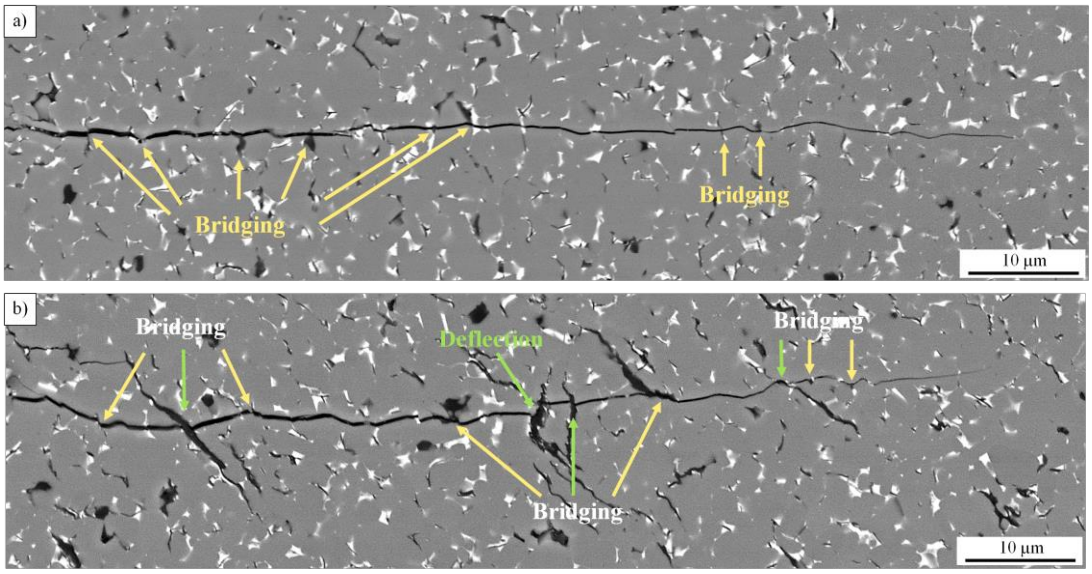

Figure 7. *Representative toughening mechanisms occurred in the (a) SiC matrix and (b) SiC matrix composite containing GPLs sonicated for 2 h in the in-plane (⊥) direction.*

It was determined that the fracture toughness values of all the GPLs containing SiC composites were higher in the in-plane direction than in the through-plane direction as consistent with studies on GPLs-ceramic matrix composites produced with SPS [19, 30]. However, the toughness differences between the two directions varied between ~ 8 and 3 %, indicating a slight anisotropy. The difference in toughness between the two directions decreased with increasing sonication time applied to the GPLs. This can be explained by the fact that it becomes more difficult for GPLs to be oriented in a particular direction in the matrix microstructure as their platelet size decreases.

2. CONCLUSION

The effects of adding the GPLs sonicated for 1, 2, 4 and 6 h on the microstructure and mechanical properties of SiC ceramics such as hardness and fracture toughness were investigated. Microstructural analyses showed that GPLs agglomerates dispersed, and the platelet size of GPLs decreased with increasing sonication time. Although this decrease in platelet size was minimal up to the 2 h sonication time, it became evident in the GPLs sonicated for 4 and 6 h. Raman analyses indicated that stacked GPLs dispersed and became thinner up to 2 h sonication time, and after this point, when the sonication time increased to 4 and 6 h, the GPLs agglomerates continued to be dispersed, but the thickness of the already thinned ones remained the same. Optimum dispersion was achieved with the least change in platelet size at 2 h of sonication. With the addition of GPLs sonicated at different times, the hardness of the SiC matrix decreased by about 5-8%. Among the GPLs sonicated at different times, the highest fracture toughness in both the through-plane and in-plane directions was obtained in the SiC containing GPLs sonicated for 2 h. The toughness of 2 h sonicated GPLs-SiC composite was higher than SiCs containing non-sonicated and 1 h sonicated GPLs because of their more homogeneous dispersion in the matrix microstructure. The higher degree of increase in fracture toughness of SiC matrix by GPLs sonicated for 2 h compared to GPLs sonicated for 4 and 6 h was due to the positive effect of larger platelet size and aspect ratio. GPLs have increased the fracture toughness of SiC matrix through bridging and deflection toughening mechanisms.

ACKNOWLEDGMENTS

This study was supported by the Eskisehir Technical University Scientific Research Projects under the project numbers of 20ADP087. The author would like to thank to Prof. Dr. Servet Turan for providing all the raw materials for the production of materials and also to Furkan Buluç and Orhan Çetin for their contributions to the study.

REFERENCES

[1] Singh, V., Joung, D., Zhai, L., Das, S., Khondaker, S.I., Seal, S. (2011). Graphene based materials: past, present and future. Prog. in Mat. Sci., 56, 1178–1271. ttps://doi.org/10.1016/j.pmatsci.2011.03.003.

[2] Mas-Balleste, R., Gomez-Navarro, C., Gomez-Herrero, J., Zamora, F. (2011). 2D materials: to graphene and beyond. Nanoscale, 3, 20-30. 10.1039/c0nr00323a.

[3] Geim, A.K., Novoselov, K.S. (2007) The rise of graphene. Nature Mat., 6, 183–191. 10.1142/9789814287005_0002

[4] Abderrezak, H., Bel Hadj Hmida, E.S. (2011). Silicon Carbide: Synthesis and Properties in Properties and Applications of Silicon carbide. IntechOpen. ISBN: 978-307-201-2.

[5] Kordina, O., Saddow, S.E. (2004). Silicon Carbide Overview in Advances in Silicon Carbide Processing and Applications. Artech House, Inc., Boston, 1-23. ISBN:1-58053-740-5.

[6] Mukasyan, A.S. (2017). Silicon Carbide, in Concise Encyclopedia of Self-Propagating High-Temperature Synthesis, History, Theory, Technology, and Products. Elsevier Science. ISBN: 9780128041888 336-338.

[7] Bodis, E., Cora, I., Balazsi, C., Nemeth, P., Karoly, Z., Klebert, S., Fazekas, P., Keszler, A.M. (2017). Spark plasma sintering of graphene reinforced silicon carbide ceramics. Ceram. Int., 43 (12), 9005-9011. https://doi.org/10.1016/j.ceramint.2017.04.042.

[8] Li, S., Luo, X., Wei, C., Gao, P., Wang, P., Zhou, L. (2020). Enhanced strength and toughness of silicon carbide ceramics by graphene platelet-derived laminated reinforcement. J. of All. and Comp., 834, 155252. https://doi.org/10.1016/j.jallcom.2020.155252.

[9] Rahman, A., Singh, A., Karumuri, S., Harimkar, S.P. (2015). Graphene reinforced silicon carbide nanocomposites–Processing and properties. Comp., Hybrid, and Multifunc. Mat., 4, 165-176. 10.1007/978-3-319-06992-0_21.

[10] Yang, Y., Li, B., Zhang, C, Wang, S., Liu, K., Yang, B. (2015). Fabrication and properties of graphene reinforced silicon nitride composite materials. Mat. Sci. and Eng.:A, 644, 90-95. https://doi.org/10.1016/j.msea.2015.07.062.

[11] Taylor, A.C. (2012). Processing of polymer nanocomposites. Manufac. Tech. for Poly. Mat. Comp. (PMCs) 95-119. https://doi.org/10.1533/9780857096258.1.95.

[12] Porwal, H., Tatarko, P., Grasso, S., Khaliq, J., Dlouhý, I., Reece, M.J. (2013). Graphene reinforced alumina nano-composites. Carbon, 64, 359-369. https://doi.org/10.1016/j.carbon.2013.07.086.

[13] Yun, C., Fenga, Y., Qiu, T., Yang, J., Li, X., Yu, L. (2015). Mechanical, electrical, and thermal properties of graphene nanosheet/aluminum nitride composites. Ceram. Int., 41(7), 8643-8649. https://doi.org/10.1016/j.ceramint.2015.03.075.

[14] Tapasztó, O., Puchy, V., Horváth, Z.E., Fogarassy, Z., Bódis, E., Károly, Z., Balázsi, K., Dusza, J., Tapasztó, L. (2019). The effect of graphene nanoplatelet thickness on the fracture toughness of Si_3N_4 composites. Ceram. Int., 45(6), 6858-6862. https://doi.org/10.1016/j.ceramint.2018.12.180.

[15] Kandemir, S. (2018). Grafen Nanolevha Takviyesinin AlSi10Mg Alaşımının Mikroyapı ve Mekanik Özellikleri Üzerine Etkisi. Gazi Üniv. Fen Bil. Derg. Part C: Tas. ve Tek., 6(1), 177-187. 10.29109/http-gujsc-gazi-edu-tr.334577.

[16] Markandan, K., Chin, J.K., Tan, M.T.T. (2017). Recent progress in graphene based ceramic composites: a review. J. of Mat. Res., 32, 84-106. 10.1557/jmr.2016.390.

[17] Muthoosamy, K., Manickam, S. (2017). State of the art and recent advances in the ultrasound-assisted synthesis, exfoliation and functionalization of graphene derivatives. Ultrasonics Sonochem., 39, 478-493. https://doi.org/10.1016/j.ultsonch.2017.05.019.

[18] Zhang, B., Chen, T. (2019). Study of Ultrasonic Dispersion of Graphene Nanoplatelets. Materials, 12(11), 1757. https://doi.org/10.3390/ma12111757

[19] Baskut, S., Cinar, A., Turan, S. (2017). Directional properties and microstructures of spark plasma sintered aluminum nitride containing graphene platelets. J. of the Europ. Ceram. Soc., 37, 3759–3772. https://doi.org/10.1016/j.jeurceramsoc.2017.03.032.

[20] Rangel, E.R. (2011). Fracture Toughness Determinations by Means of Indentation Fracture, Nanocomposites with Unique Properties and Applications in Medicine and Industry. InTech. ISBN:978-953-307-351-4.

[21] Ferrari, A.C. (2007). Raman spectroscopy of graphene and graphite: disorder, electronphonon coupling, doping and nonadiabatic effects. Solid State Comm., 143, 47–57. https://doi.org/10.1016/j.ssc.2007.03.052.

[22] Li, C., Li, D., Yang, J., Zeng, X., Yuan, W. (2011). Preparation of single- and few-layer graphene sheets using Co deposition on SiC substrate. J. of Nanomat., 2011, 319624. doi:10.1155/2011/319624.

[23] Childres, I., Jaureguib, L.A., Park, W., Cao, H., Chen, Y.P. (2013). Raman spectroscopy of graphene and related materials. 97, 173109.

[24] Ramirez, C., Garzon, L., Miranzo, P., Osendi, M.I., Ocal, C. (2011). Electrical conductivity maps in graphene nanoplatelets/silicon nitride composites using conducting scanning force microscopy. Carbon, 49, 3873–3880. https://doi.org/10.1016/j.carbon.2011.05.025.

[25] Turan, S., Knowles, K.M. (1995). High resolution transmission electron microscopy of the planar defect structure of hexagonal boron nitride. Phy. Status Solidi (a), 150, 227-237. https://doi.org/10.1002/pssa.2211500120.

[26] Moslemi, M., Razavi, M., Zakeri, M., Rahimipour, M.R., Schreiner M. (2018). Effect of carbon fiber volume fraction on 6H to 4H-SiC polytype transformation. Phase Transitions, 91 733–741. https://doi.org/10.1080/01411594.2018.1481214.

[27] Chatterjee, S., Nafezarefi, F., Tai, N.H., Schlagenhauf, L., Nüesch, F.A., Chu, B.T.T. (2012). Size and synergy effects of nanofiller hybrids including graphene nanoplatelets and carbon nanotubes in mechanical properties of epoxy composites. Carbon, 50, 5380–5386. https://doi.org/10.1016/j.carbon.2012.07.021.

[28] Halpin, J. (1969). Stiffness and expansion estimates for oriented short fiber composites. J. of Comp. Mat., 3(4), 732-734. https://doi.org/10.1177/002199836900300419.

[29] Mori, T., Tanaka, K. (1973). Average stress in matrix and average elastic energy of materials with misfitting inclusions. Acta Metall, 21(5) 571-574. https://doi.org/10.1016/0001-6160(73)90064-3.

[30] Tapasztó, O., Puchy, V., Horváth, Z.E., Fogarassy, Z., Bódis, E. (2019). The effect of graphene nanoplatelet thickness on the fracture toughness of Si_3N_4 composites. Ceram. Int., 45(6), 6858-6862. https://doi.org/10.1016/j.ceramint.2018.12.180.